Journal of Physics: Conference Series

PAPER • OPEN ACCESS

Enhancing airport runways performance using composite systems numerically using unit cell concept.

To cite this article: A. M. Abdelaziz *et al* 2023 *J. Phys.: Conf. Ser.* **2616** 012052

Enhancing airport runways performance using composite systems numerically using unit cell concept.

A. M. Abdelaziz[1], Ahmed Elsheseny[1], Nabil Abdelmotaal[1], and Nabil M. Nagy[1].

[1] Civil Engineering Department, Military Technical College, Cairo, Egypt.

Emails: abdelazizmohamed@mtc.edu.eg

Abstract. One of the problems, which would affect airport runways is the settlement of soil. Such settlement would be controlled by enhancing the performance of the soil underneath the airport runway. The composite system consists of graded stone-reinforced soil and reinforcing layers. This system is defined as stone column, which is widely used to improve weak soils as one of the soil stabilization methods due to its simple construction and economic cost. It is used to reduce settlement and enhance soil-bearing capacity. By using such technique, part of the high-compressibility and low-shear strength soil is replaced with coarse filler materials with high-shear strength and extremely low compressibility. In this study, a 3D numerical model of a unit cell is created to examine the impact of changing the controlling parameters in the model, i.e. spacing between columns (S), weak soil cohesion (c), and angle of internal friction for stone column material (φ). It was established that the use of stone columns improves the soil-bearing capacity and reduces settlement, strengthening the stability of airport runways. The efficiency of the system is improved by increasing the column material's internal friction angle and the cohesion of the surrounding soil. The ultimate bearing capacity of soil without SC and SC-soil systems were 150 kPa, and 460 kPa, respectively, which illustrates that the bearing capacity was increased by 306.7%.

1. Introduction:

One of the main problems associated with using soft soils is their high compressibility and low shear strength. Such soil would cause catastrophic problems, i.e. failure of the above structures or lack of structures serviceability, if used as base soil underneath strategic constructions, such as airports, skyscrapers, high-rise buildings, … etc. [1]. In order to avoid such problem, two solutions could be adopted, replacing the construction location or improving the base soil performance under applied loads. Recently, soil improvement has been proven to be economical method compared with location replacement, where some locations have strategic importance. There are various methods for soil improvement such as lime treatment, soil cement column, soil nailing, vacuum pre-consolidation, geosynthetic reinforcement [2, 3], deep compaction, pre-consolidation using stone columns, or pre-fabricated vertical drains. In this study stone columns, SC, are used to improve weak soil. SC are typically filling soil or rocks of higher properties, in particular the shearing strength, compared with the surrounding weak soil. After inserting SC, a composite system, i.e. native weak soil in addition to filling soil, of higher properties is generated. SC has variable benefits for the overall system, where it is easy to be constructed, enhances the bearing capacity, controls foundation total and differential settlement, and accelerates both the drainage rate and soil consolidation. Generally, the load transfer from the SC to the surrounding weak soil would occur as a result of shear stresses at the interaction and end bearing at the base of the SC. Therefore, the behavior of SC could be the same as that of a pile, regardless of the bulging, which occurs in the SC [4], as presented in Figure 1.

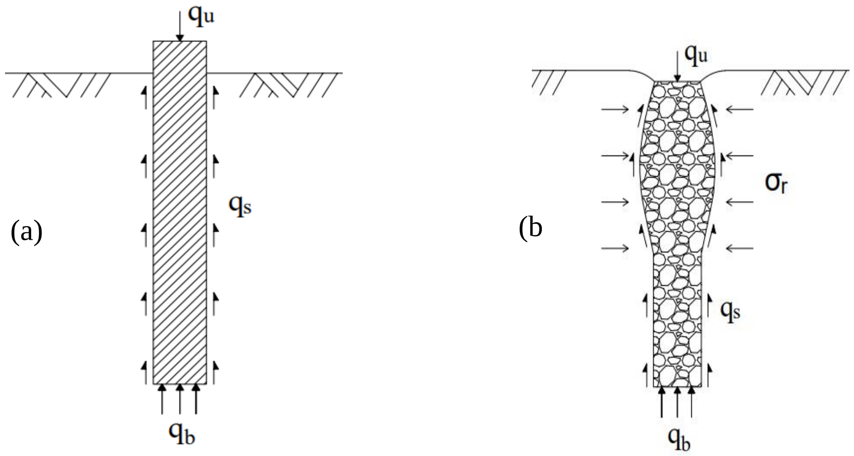

Figure 1. Load transfer mechanism for (a) a stiff rigid pile and (b) a stone column (McCabe, McNeill and Black [4]).

Ambily and Gandhi [5], and Kumar and Jain [6] investigated the behavior of SC numerically and experimentally. They investigated the variation of different ratios for the spacing between SCs to the diameter of the SC, S/d ratios, cohesion of native soil, and its water content on the performance of system. It was concluded that S/d of 4 is not noticeably enhancing the load-settlement when compared to S/d of 2 and 3, and the bearing capacity of SC decreases as the moulding water content increases. Furthermore, increasing the stone column diameter significantly enhanced the bearing capacity of weak soil. The effect of varying the diameter of SC, and the compactive energy applied to it, on the overall performance of SC-reinforced soil was examined by small-scale experiments, Chandrawanshi, Kumar and Jain [7]. It was reported that installing SCs significantly decreased the settlement of soft clay bed. On the other hand, increasing the compactive energy applied on SCs resulted in significant reduction in soil settlement, while fixing the diameter of SCs. The impact of varying S/d and the undrained shear strength of soil bed, on the load-settlement response was experimentally investigated, Almaliki and Selamat [8]. It was reported that the ability of SC to support loads was found to be directly related to the undrained shear strength of soil and inversely proportional to S/d. When undrained shear strength and S/d increased and decreased, respectively, the load-bearing capacity was improved. The influence of replacing a ratio of the SC material with quarry dust, where the whole SC was wrapped with geotextiles was investigated experimentally, Beena [1]. It is revealed from the studies that a portion of stone, 30% by weight, can be replaced by cheaper quarry dust without affecting the performance of the system.

The performance of a group of SCs beneath a uniformly loaded area representing loads resulting from an airport runway pavement, could be simplified by investigating the behaviour of one column in the middle of a cylindrical soil bed, which would represent the zone of influence of the column, i.e. unit cell concept, Figure 2. Integrating multiple unit cells would represent the overall performance of the SC-reinforced soil. In this study ABAQUS software was utilized to generate a 3D numerical model for a unit cell to study the effect of changing the controlling parameters in SC-reinforced soil system mainly, S/d, the stone column material internal angle of friction (φ), the cohesion of native soil (c), and the existence of geosynthetic encasement around SC material, ESC.

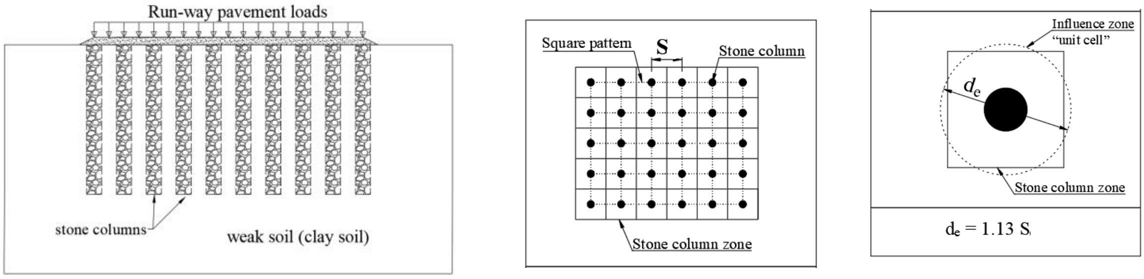

a) Soil improved profile b) SCs pattern c) Unit cell

Figure 2. unit cell simplification.

2. Numerical Analysis:

One of the most important advantages of finite element package ABAQUS is its durability in the numerical approach for resolving soil nonlinearity [9-12]. So, in this study (ABAQUS/ CAE 2017) was used to investigate SC influence in improving weak soils. To properly model weak soil and SC, proper consideration for both the geometry and the constitutive model should be followed.

2.1. Geometry Model

To study the overall performance of soil reinforced with SC beneath the pavement of a runway, unit cell concept was used numerically. As shown in Figure 3, the unit cell consists of a single SC in the middle of a cylindrical soil, which has a diameter representing the unit cell effective diameter, d_e. Effective diameter of unit cell is a parameter depends on the spacing and the pattern of SCs. In the current research, and according to the used pattern, i.e. square pattern, the value of d_e was chosen as 1.13 S [13] . The model composed of a SC with constant diameter of 100 mm and constant length of 450 mm. It was considered that the length of the SC is shorter than that of the soil, which allows transferring the generated stresses between them through only friction as bedding soil is weak one with low bearing capacity, i.e., floating SC. Parametric study was carried out on the constructed model, while changing the column material strength and cohesion of native soft soil. In this research, the ratio between the spacing between SC and its diameter was investigated, where it varied between S/d = 2,3,4, and 5.

2.2. Material modelling

Three-dimensional modelling of the soil and SC is performed, while using eight-node continuum brick elements with reduced integration (C3D8R) as element type. Furthermore, four-node shell elements with reduced integration (S4R) is used for encasement material, as shown in Figure 3. Stone columns and the soft soil were modelled and idealized using Mohr-Coulomb (MC) model [14]. It should be observed that the Mohr-Coulomb criteria failure depends on both the normal and shear stresses that are created in the soil in the same plane. The Mohr-Coulomb concept is based on Mohr's circle represented by the plane of the maximum and minimum principal stresses for states of stress at failure. The material properties used in this numerical study are illustrated in Table 1.

Table 1. The properties used in the study for modelling soil, stone column and encasement.

properties	Weak soil (soft clay)	Stone column material	Encasement
Elastic material, E (MPa)	5.5	55	263
Poisson's ratio, μ	0.42	0.30	0.30
Density, γ (KN/m^3)	19.83	16.95	75.0
Internal friction angle, φ (°)	---	30.0, 35.0, 40.0, 45.0	---
Dilation angle, ψ (°)	---	(φ - 30°) [15]	---
Cohesion, c (MPa)	10, 15, 20, 25, 30, 35, 40	---	---

2.3. Boundary Conditions

The bottom and vertical faces of the unit cell model have boundary constraints placed on them. All nodes at the base of the model were fixed and were prevented from moving in both the vertical and radial directions, and all nodes on the vertical faces were prevented from moving in the radial direction, i.e. roller support, which allows the soil to move vertically. The roller support can refer to the provided lateral support from the cells beside the investigated one, which will prevent the lateral movement of the soil. The upper surface was left unrestricted to allow its movement. Figure 3. shows the 3D model after applying the boundary conditions.

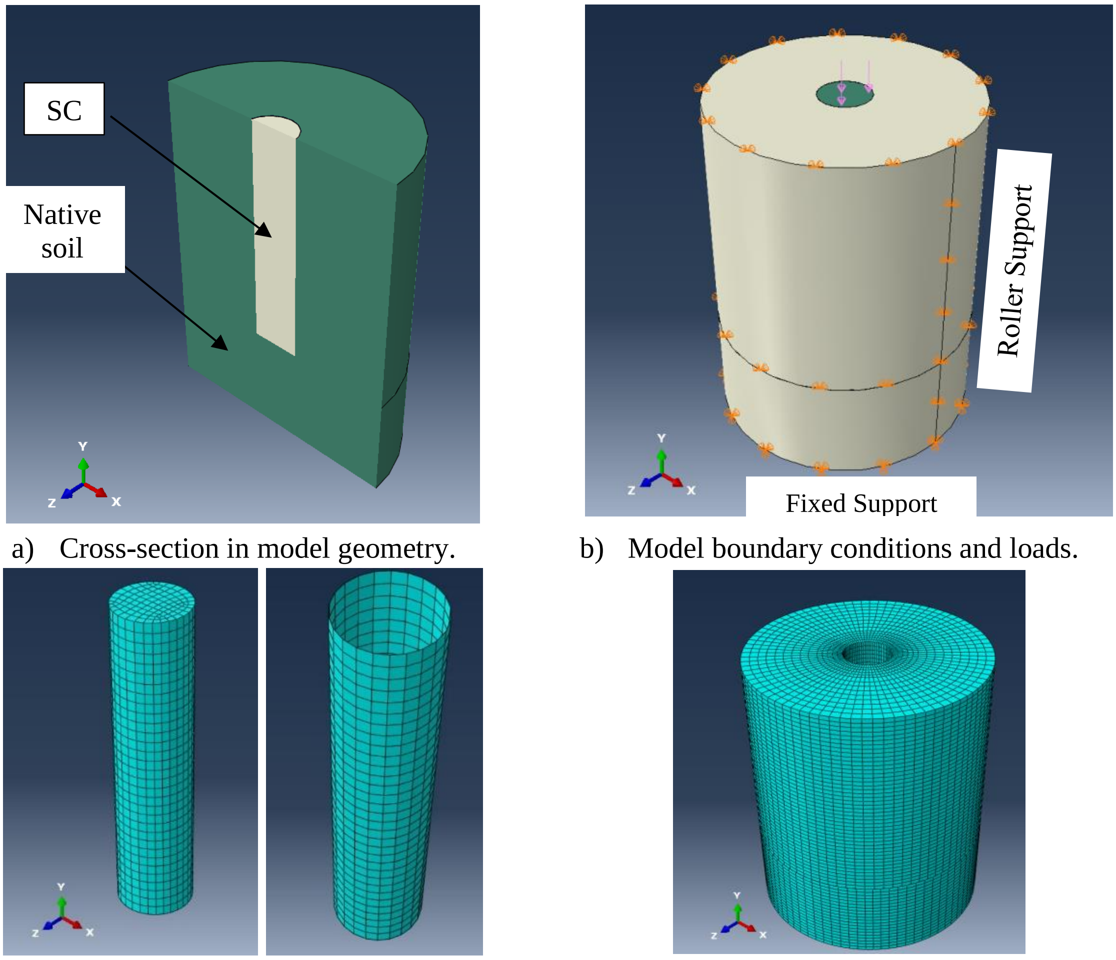

a) Cross-section in model geometry.

b) Model boundary conditions and loads.

c) Stone column and encasement meshing.

d) Native soil meshing.

Figure 3. Numerical analysis parameters.

2.4. Loads

While constructing runway over weak soil, the load is transferred to the soil through the contact area between the wheel of the plane and the surface layer of the runway. It should be noted that SCs reinforce the weak soil, which is located under the top layer of the runway. Therefore, the load is redistributed through the surface layer and is transferred to the SC-reinforced soil. Consequently, the load is mitigated and redistributed over a wider area compared to the contact area between the wheel and the surface layer. According to FWA [16], wheel loads transmitted to the soil beneath the pavement as a distributed load at specified depth depending on the type of pavement as shown in Figure 4. In addition, geostatic pressure was applied using gravity load in the vertical direction [10]. However, the numerical study did not take into account the stress generated by the column installation technique.

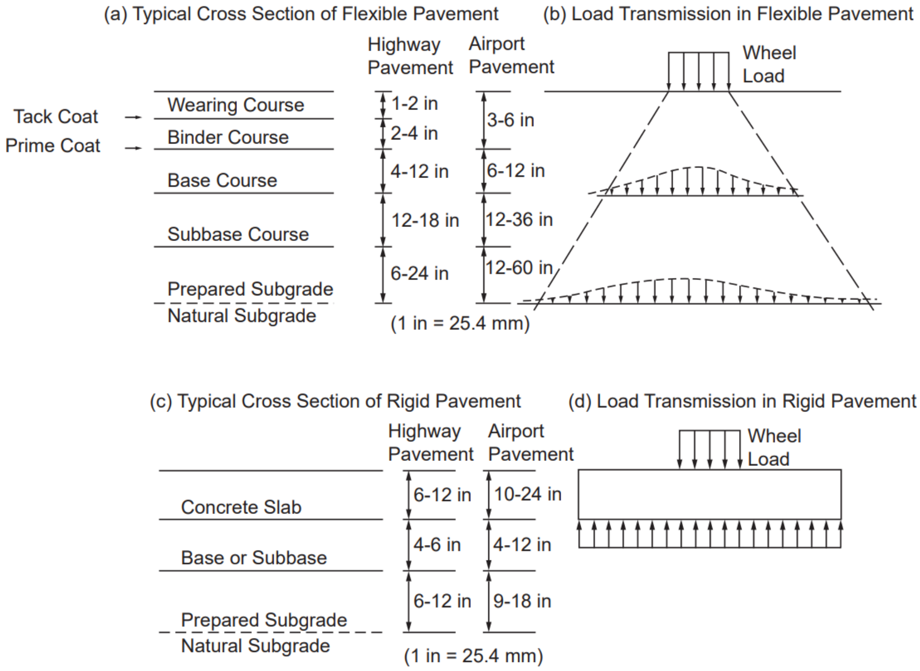

Figure 4. Load transmission in flexible and rigid pavements for highways and airports, Fwa [16].

2.5. Meshing

To model the soil and stone column, eight-node continuum brick elements with reduced integration (C3D8R) were implemented. A four-node shell element with reduced integration (S4R) was used for encasement. The mesh was performed considering an aspect ratio, which didn't exceed 2.5. Sensitivity analysis for mesh size was performed until reaching the optimum mesh size. The optimum mesh was selected where the accuracy of the results was almost constant while reducing the element size [12].

2.6. Interaction

The model consists of SC and weak soil. Consequently, two interaction surfaces were generated. The first surface between the radial area between SC and the soil, and the second surface between the base of SC and the soil beneath it. Frictional interaction should be defined between the interacted materials. However, due to the difficulty of defining the friction coefficient between both of them, which mainly requires performing an experimental large direct shear test and replacing the upper part of the soil by the SC material, for each SC and weak soil materials. Therefore, tie interaction was adopted in the model, which ensure that all the nodes of the SC are connected to those of the soil [17]. The material which has coarser mesh and higher stiffness was defined as the master surface in the contact pair [18]. For ESC, the interaction between the encasement and the column materials was represented as an embedded region.

3. Model Validation:

The validation of the developed numerical model was carried out considering the experimental and numerical models performed by Ambily and Gandhi [19]. In a special cylindrical tank with 420 mm diameter and 500 mm height, the experimental model was tested. Crushed stone aggregates were used to construct SC, and clay, which is classified as CH, was used as soft soil. Table 2 summarizes the properties of the used materials. Experimentally, SC was constructed by replacement method, and loading was applied on a small steel plate, representing the footing, with the same diameter of the SC, 100 mm. Figure 5 shows the results of the validation. Good agreement between the numerical and experimental result was obtained. On the other hand, the obtained numerical results had slight variation compared with those provide by [19], where the geostatic pressure effect was considered in the ABAQUS analysis.

Table 2. The properties of the used materials in validation.

Material	w (%)	E (KPa)	υ	c_u (KPa)	ψ (deg.)	φ (deg.)	γ (kN/m^3)
Clay	25	5500	0.42	30	---	---	19.45
Stone	---	55000	0.3	---	10	43	16.62

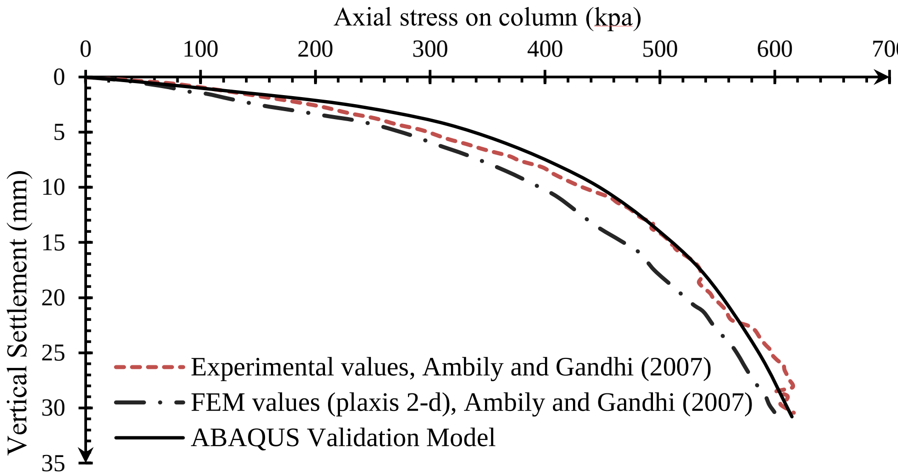

Figure 5. The results of the validation.

4. Parametric study and discussion:

4.1. Evaluating system performance

The behavior of the system was numerically investigated to assess the load-settlement behavior of the stone column and investigate its failure mechanism. The composite system of SC-soil model was constructed representing unit-cell concept. To demonstrate the improvement achieved by installing SCs, the results were compared to the case of only soil, i.e. unreinforced soil without stone column, as shown in Figure 6. It is clearly illustrated that the use of SCs improve the load-settlement performance by enhancing load bearing capacity and reducing settlement. The ultimate bearing capacity of soil without SC and SC-soil systems were 150 kPa, and 460 kPa, respectively, which illustrates that the bearing capacity was increased by 306.7%.

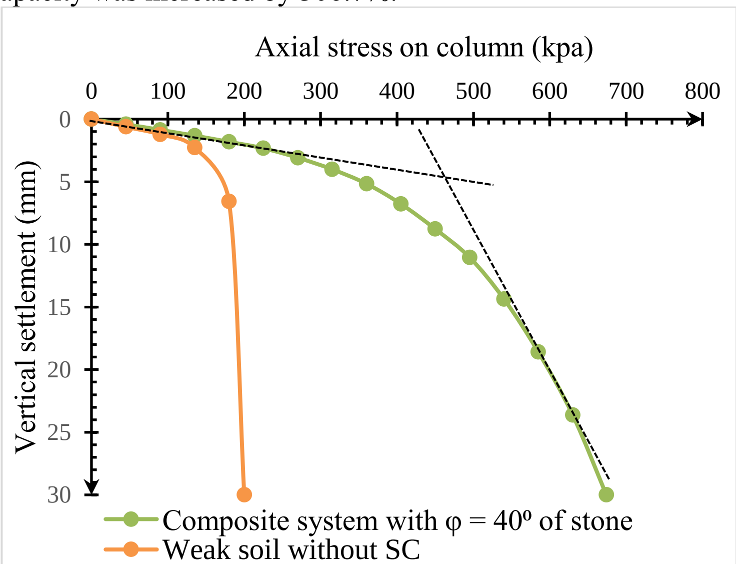

a) Lod-settlement behaviour of SC.

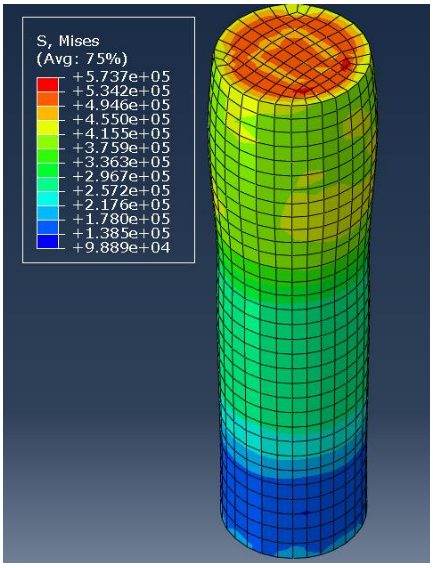

b) Stresses on the SC.

Figure 6. Load-settlement behaviour of soil without SC and with SC.

The ultimate bearing capacity was calculated according to approximate formula suggested by Hugher and Withers [20], to compare the numerical results with analytical results, and was found to be 415 KPa, Equation (1). According to the model results, the main failure was introduced by the column bulging, as presented in Figure 7. It was noticed that the column bulging occurred in the top section of the column (2d), and the maximum bulging observed at a depth of (d) from the column top. This bulging can be reduced by using geosynthetic encasement.

$$q_a = \frac{K_p}{SF}(4c + \sigma`_r) \qquad \text{Equation (1)}$$

Where: K_p is the passive earth pressure coefficient, $K_P = tan^2(45^o + \frac{\Phi`}{2})$, Φ` is the drained angle of internal friction of stone (40 degree), c is drained cohesion (15 KPa) and $\sigma`_r$ is effective radial stress as measured by a pressure meter (2c if pressure meter data are not available).

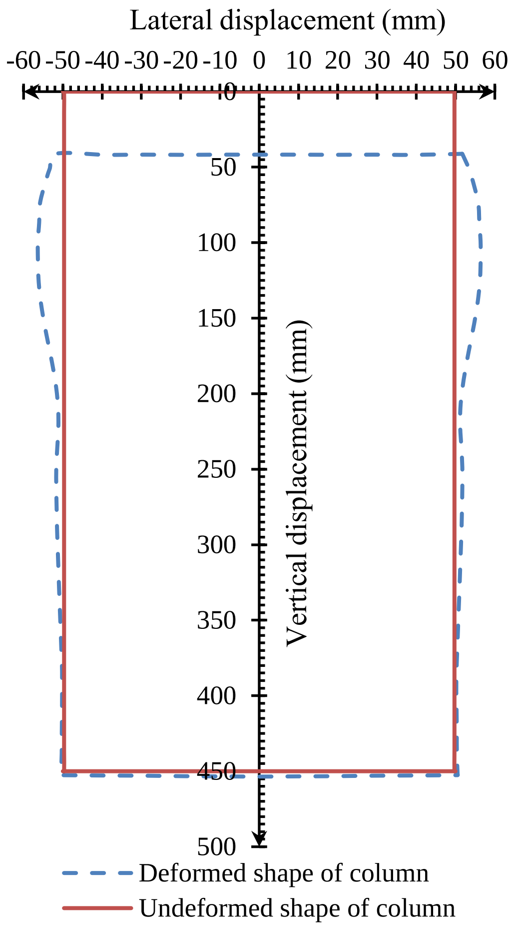

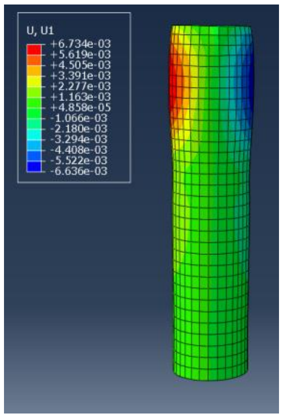

b) lateral displacement contour.

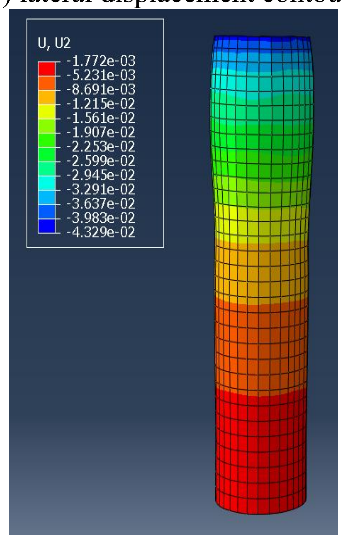

a) Undeformed shape of column. c) Vertical displacement contour.

Figure 7. Deformed shape of SC and its main failure mode.

4.2. Effect of S/d ratio

Figure 8 shows the stress-settlement response of the SC, while varying S/d. It is obvious that decreasing S/d ratio significantly contributed to increasing the axial stress capacity of the system before failure occurrence. This could be attributed to the enhanced lateral confining pressure provided by the surrounding soil because of the decrease of the spacing between SCs. Furthermore, the contribution of varying S/d became observable at significantly increased load, where the response was almost identical until reaching axial load of 220 kPa. Consequently, the contribution of varying S/d would be remarkable at relatively higher applied loads, where frictional load transfer mechanism occurs.

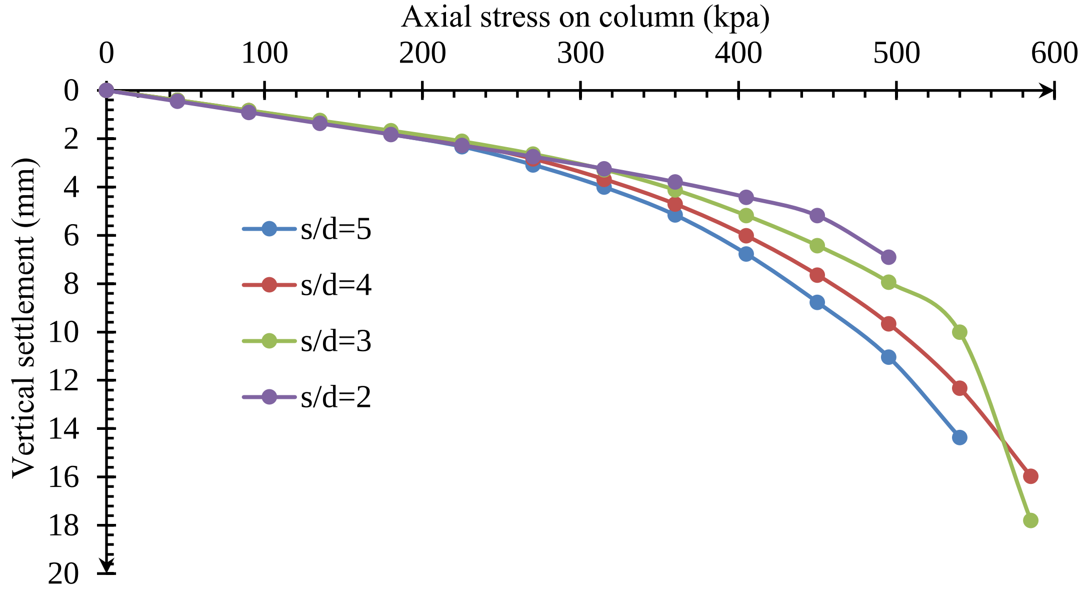

These values were taken at the center of the top surface of the SC.
Figure 8. Load settlement response of variable S/d ratio.

4.3. Effect of internal friction angle of SC

Figure 9 demonstrates the stress-settlement response of SC-reinforced soil while varying the internal friction angle from 30º to 45º. It can be observed that increasing of friction angle of SC material significantly contributed to enhancing the load-capacity of the system, where it was 270 kPa and 570 kPa while using friction angle of 30º and 45º friction angles, respectively at the same settlement. Furthermore, the increase of the friction angle contributed to increase the stiffness of the SC, which by turn contributed to decreasing the occurred bulging in the SC. Figure 10 illustrates the occurred lateral bulging of the SC while varying its internal friction angle. Such response supports that increasing the friction angle contributes to decreasing the lateral displacement of SC, as its stiffness increases, which decreases its bulging. From numerical parametric study, it is observed that the lateral displacement reduced from 1.60 mm when friction angle is 30º to 0.30 mm with column friction angle of 45º.

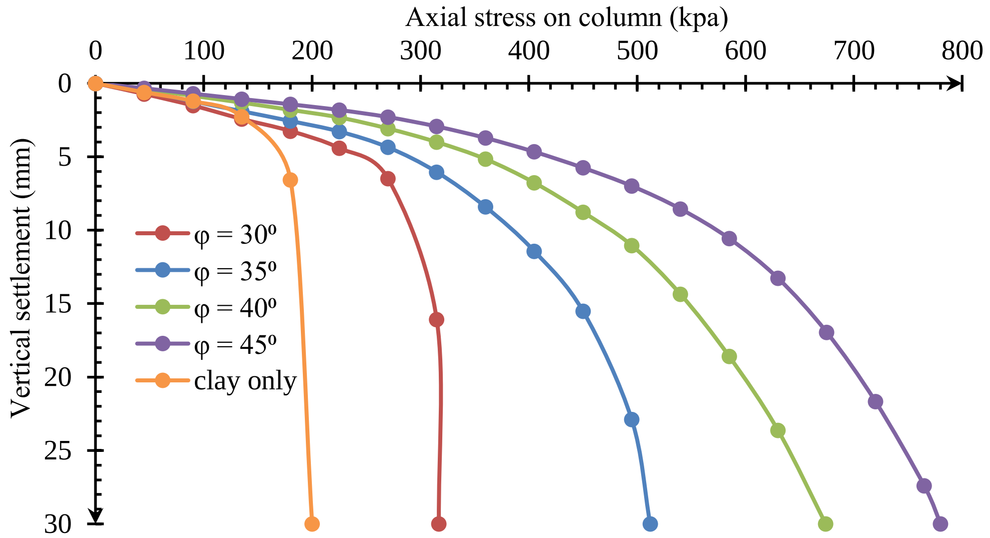

These values were taken at the center of the top of the SC and soil cohesion is constant (c = 30 kpa)
Figure 9. Load-settlement of SC-reinforced soil with different SC internal friction angle.

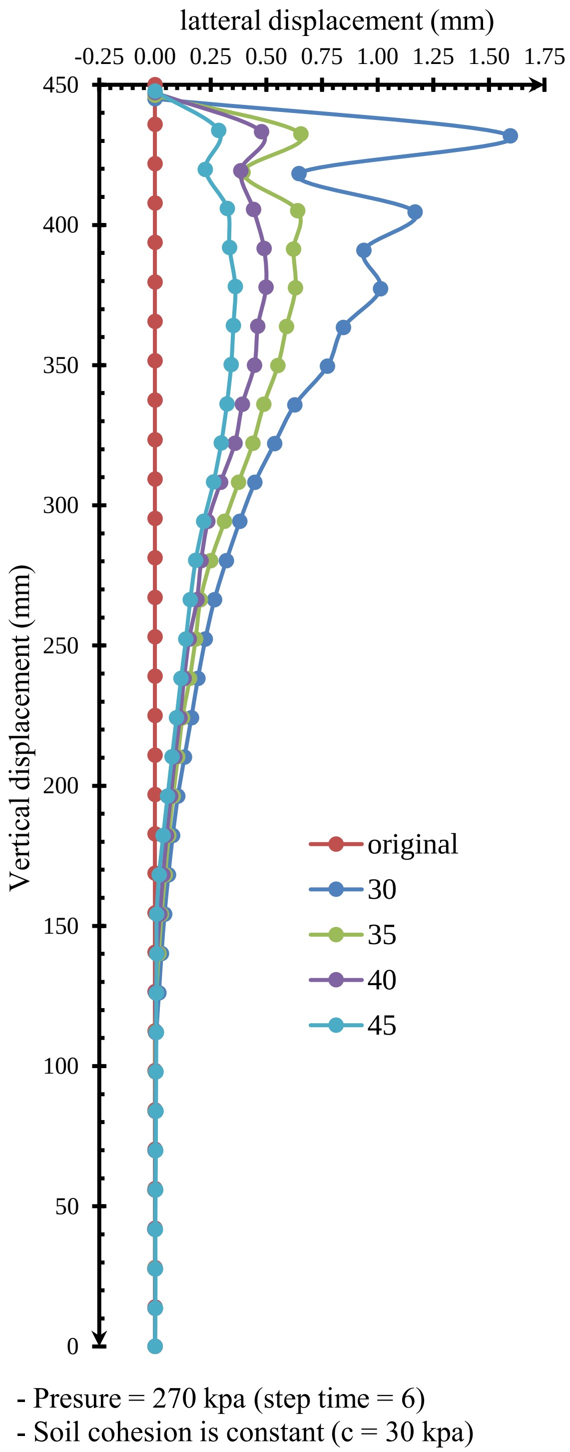

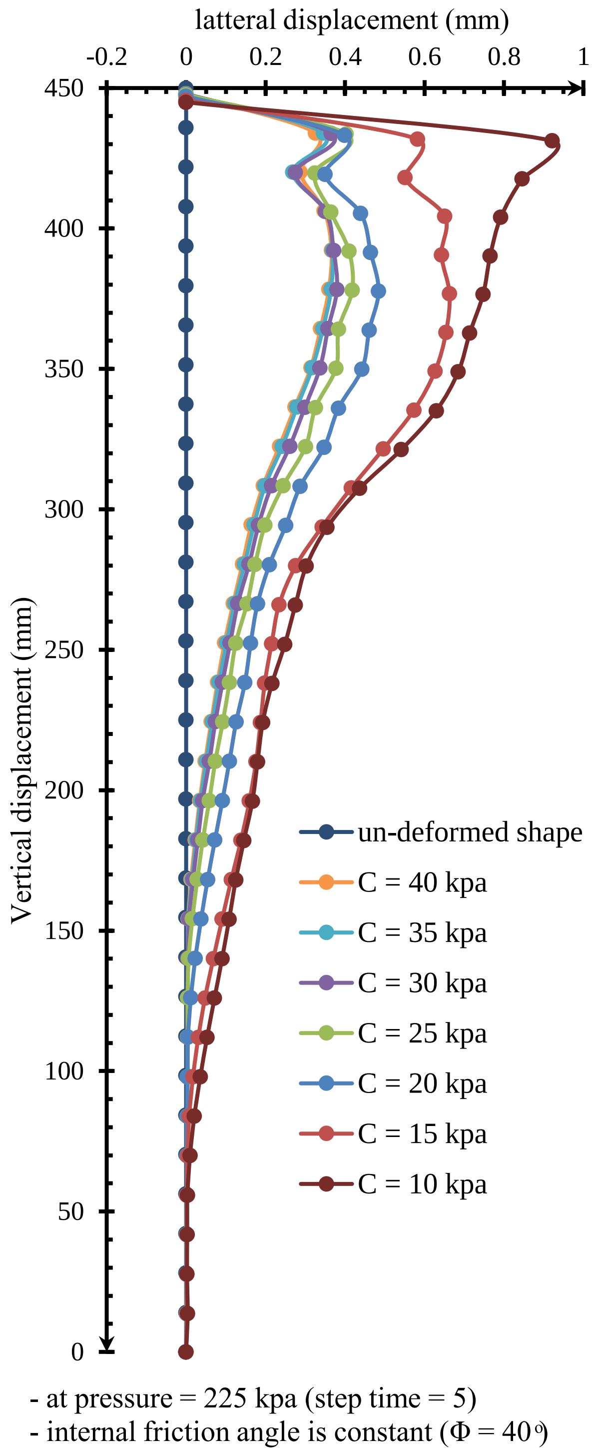

a) with variable column material friction angle. b) with variable cohesion of surrounding soil.

Figure 10. SCs lateral displacement (bulging shape of column).

4.4. Effect of cohesion of native soil

The cohesion value of native soil significantly influences the load bearing carrying of the soil reinforced with SC. Figure 11 illustrates load-settlements of the system while varying the cohesion of the weak native soil. Increasing the native soil cohesion significantly enhance the ultimate bearing capacity of the SC-reinforced soil. The load-carrying capacity increased by 250%, when the native soil cohesion increased from 10 to 40 KPa. Moreover, the bulging of SC decreased as the cohesion of the soil increased, as presented in Figure 10. It is clear that the lateral displacement reduced from 0.92 mm to 0.40 mm, while changing the cohesion of native soil from 10 kPa to 40 kPa, respectively.

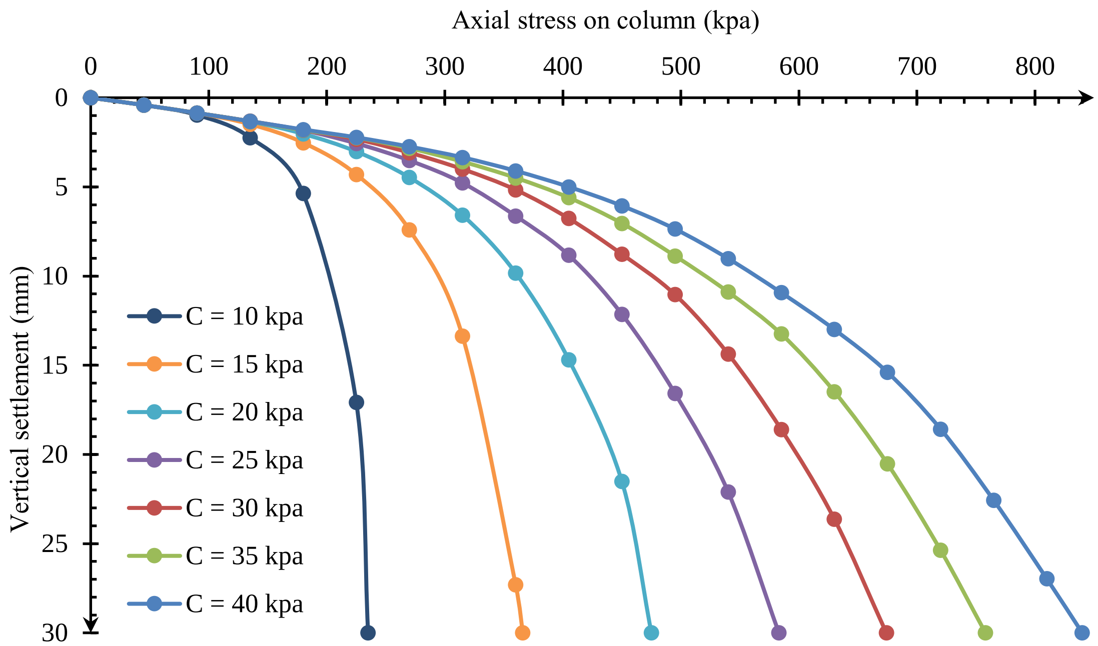

These values were taken at the center of the top surface of the SC and internal friction angle is constant ($\varphi = 40^{\circ}$)

Figure 11. Load-settlement of SC-reinforced soil with changing the cohesion of native soil.

4.5. Effect of encasement

Wrapping geosynthetic reinforcement around the SC would enhance its performance. Such behavior was observed in the ultimate bearing capacity of the system, its settlement, as well as the failure mode of the SC, which changed from only bulging into punching and reduced degree of bulging, as presented in Figure 12. Using geosynthetic ESCs allowing it to act as an end-bearing element. That would make SC act as a semi-rigid one, due to the increase in the column stiffness [21]. Figure 13 and Figure 14 present the load settlement behaviour of ESC comparing with SC, and the lateral displacement of SC and ESC, respectively.

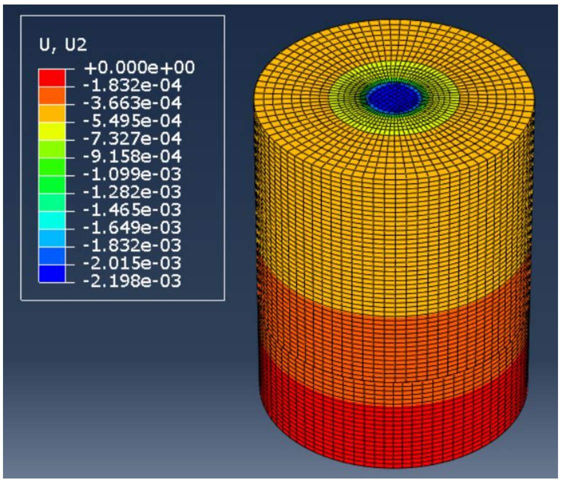

a) Settlement of overall system of ESC.

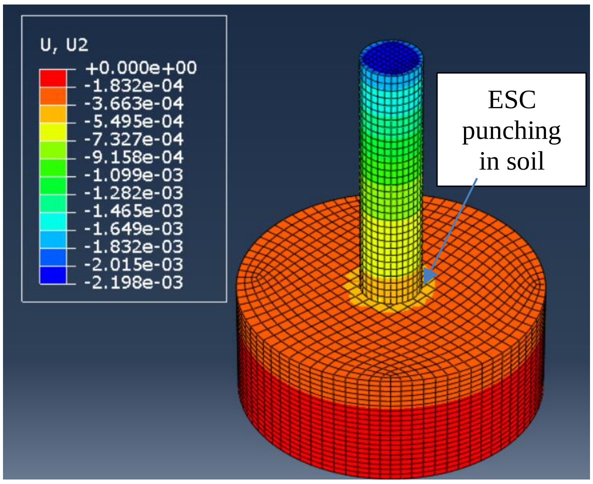

b) Settlement of the ESC toe in soil.

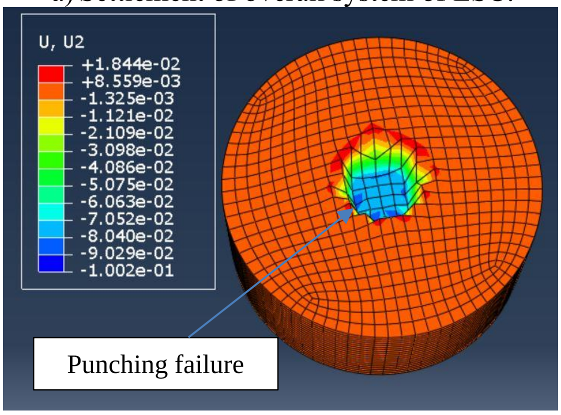

c) Punching failure of system.

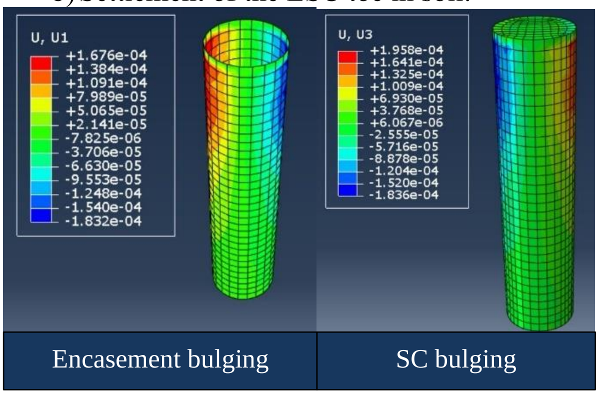

d) Lateral displacement contour of ESC.

Figure 12. settlement and failure mode of ESC.

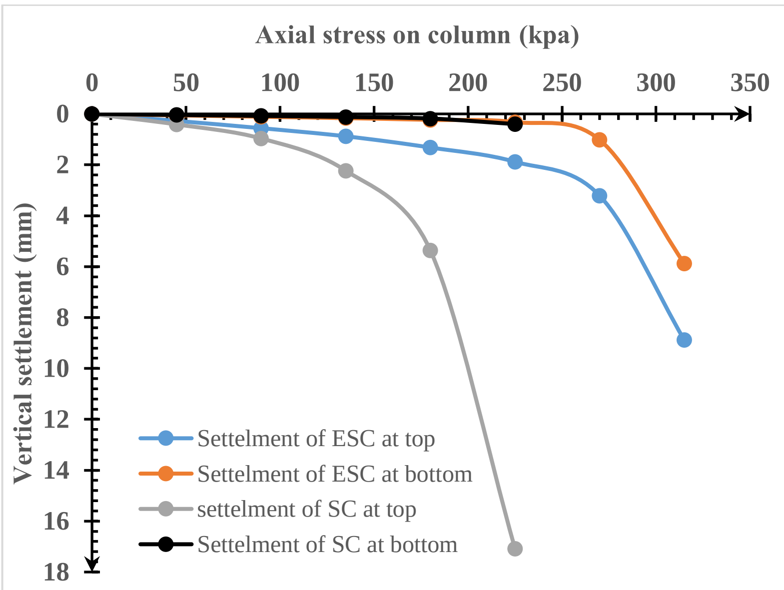

a) Lod-settlement behaviour of SC and ESC.

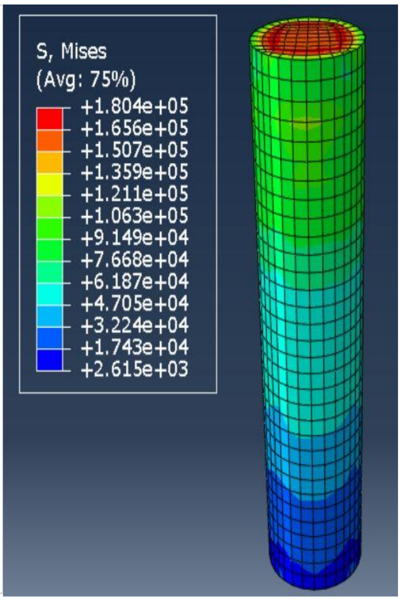

b) Stresses on the ESC.

Figure 13. load-settlement of SC-reinforced soil and ESC-reinforced soil.

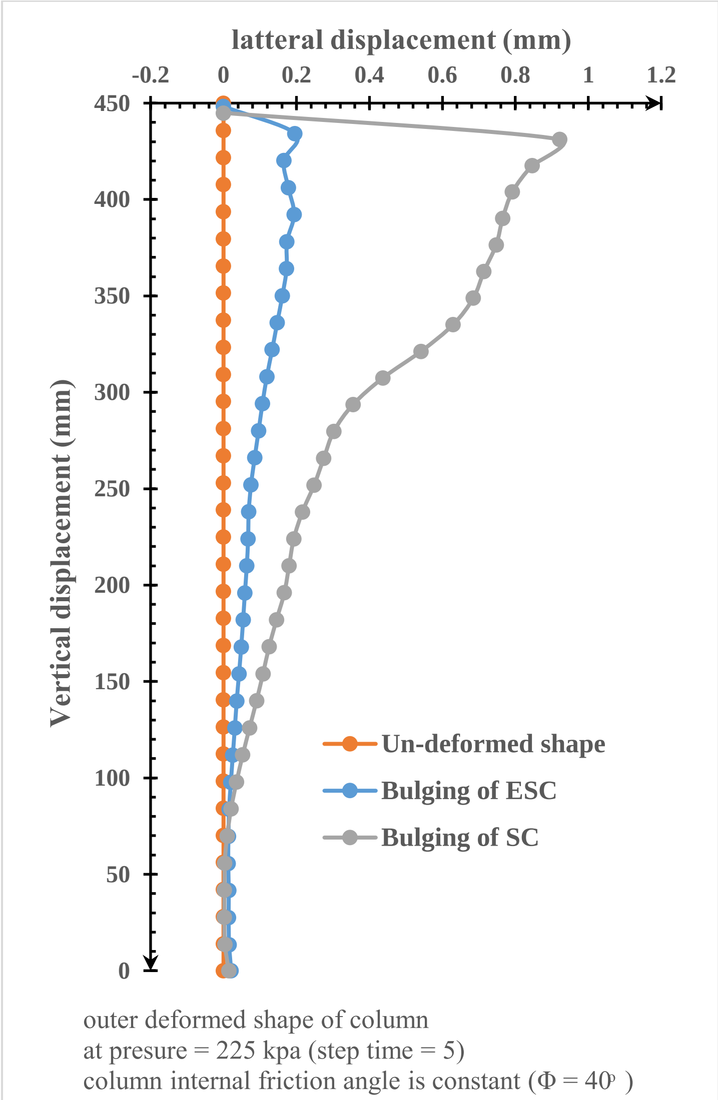

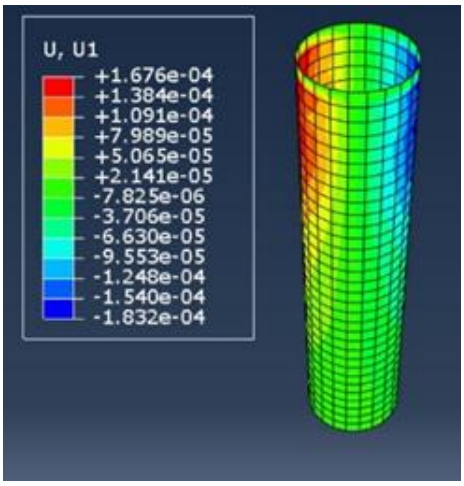

Encasement bulging

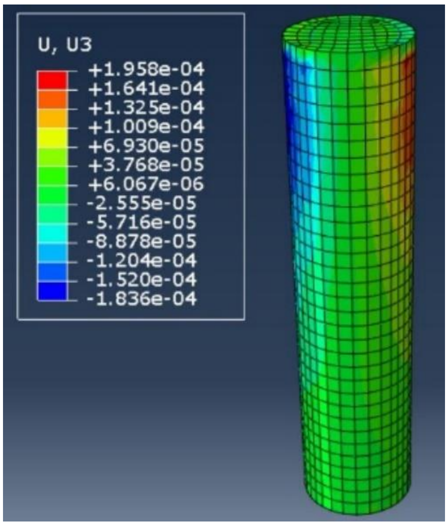

Stone column bulging

Figure 14. SC and ESC lateral displacement (bulging shape of column).

5. Conclusion:

In this paper the performance of the SC-reinforced weak soil was numerically investigated, while varying S/d, friction angle of SC, and the cohesion of native weak soil. The load-settlement behaviour and the type of system failure was numerically investigated. The following conclusions can be drawn:

- Using SC to reinforce weak soil significantly contributed to increasing its performance, which enhanced its bearing capacity, and reduced occurred settlement.
- SC-reinforced soil has variable failure mechanisms, however, in the current study bulging failure occurred.
- While using ESC, the bearing capacity and the settlement of the system increased and decreased, respectively. Furthermore, the bulging of the SC was significantly decreased, and the main failure mechanism of SC changed from bulging failure into punching failure.

- Increasing the native soil cohesion significantly enhance the ultimate bearing stress of the SC-reinforced soil. The load-carrying capacity increased by 250%, when the native soil cohesion increased from 10 to 40 KPa.

- Decreasing the spacing between SCs had a vital role to increase the load capacity of the system, which became remarkable at relatively high applied loads. Such loads have the ability to mobilize the load transfer mechanism between SC and weak soil.

- Using high quality materials of higher shear strength as a SC filling material, particularly its internal friction angle, has significant role to minimize the system settlement and hinder the bulging of SC. The lateral displacement of SC was reduced from 1.60 mm to 0.3 mm, when friction angle of SC material increased from 30^{o} to 45^{o}.

- Increasing the cohesion of surrounding native soil positively enhanced the pressure-settlement behaviour of the system. Furthermore, it decreased the bulging of column.

References
[1] Beena K, "Ground improvement using stone column," 2010,
[2] El-Shesheny A, Nagy N M, Belal A and Badawy A, "Finite element analysis of square footing resting on geosynthetic reinforced soil," 2014,vol. **10**, no. 10, pp. 1-11:Military Technical College.
[3] Abd El-Rahman A, Kamal I M, Nagy N M and Hassan M A, "Finite element analysis of reinforced sand under circular footing," 2020,vol. **974**, no. 1, p. 012004:IOP Publishing.
[4] McCabe B A, McNeill J A and Black J A, "Ground improvement using the vibro-stone column technique," 2007,
[5] Ambily A and Gandhi S, "Experimental and theoretical evaluation of stone column in soft clay," *ICGGE*, 2004,pp. 201-6.
[6] Kumar R and Jain P, "Load-Settlement Behavior of Geogrid Encased Granular Pile in Soft Expansive Soil,"
[7] Chandrawanshi S, Kumar R and Jain P, "Settlement characteristics of soft clay reinforced with stone column: an experimental small scale study," *International Journal of Civil Engineering Technology*, 2017,vol. **8**, no. 5, pp. 937-48.
[8] Almaliki B A and Selamat M R, "Behaviour of single stone columns in silty soil beds and load carrying improvement evaluation," 2017,vol. **1892**, no. 1, p. 030007:AIP Publishing LLC.
[9] Yoo C, "Interaction between tunneling and groundwater-numerical investigation using three dimensional stress-pore pressure coupled analysis," *Journal of Geotechnical Geoenvironmental engineering*, 2005,vol. **131**, no. 2, pp. 240-50.
[10] Belal A, Nagy N M and Elshesheny A, "Numerical evaluation of bearing capacity of square footing on geosynthetic reinforced sand," 2015,pp. 1-9:
[11] Nagy N M, "Numerical analysis of soft clay performance reinforced by geosynthetics encased stone columns," 2013,vol. **1558**, no. 1, pp. 1995-8:American Institute of Physics.
[12] Elshesheny A, Mohamed M, Nagy N M and Sheehan T, "Numerical behaviour of buried flexible pipes in geogrid-reinforced soil under cyclic loading," *Computers Geotechnics*, 2020,vol. **122**, p. 103493.
[13] Balaam N and Booker J, "Analysis of rigid rafts supported by granular piles.," *International journal for numerical analytical methods in geomechanics*, 1981,vol. **5**, no. 4, pp. 379-403.
[14] Malekpoor M R and Poorebrahim G, "Behavior of Compacted Lime—(Well-graded) Soil columns: Large scale tests and numerical modelling.," *Journal of Civil Engineering*, 2015,vol. **19**, no. 4, pp. 893-903.
[15] Tafreshi S M and Khalaj O, "Laboratory tests of small-diameter HDPE pipes buried in reinforced sand under repeated-load," *Geotextile Geomembranes*, 2008,vol. **26**, no. 2, pp. 145-63.

[16] Fwa T, "Highway and airport pavement design," *The civil engineering handbook*, 2003,
[17] Salam M A and Wang Q, "Numerical study on bearing capacity and bulging of the composite stone column," *The Open Civil Engineering JournaL*, 2021,vol. **15**, no. 1,
[18] Abaqus, "Abaqus 6.11," *Dassault Systemes Simulia Corporation, Providence, RI, USA* 2011,
[19] Ambily A and Gandhi S, "Behavior of stone columns based on experimental and FEM analysis," *Journal of geotechnical geoenvironmental engineering*, 2007,vol. **133**, no. 4, pp. 405-15.
[20] Hugher J and Withers N, "Reinforcing of soft cohesive soils with stone columns," *Ground engineering*, 1974,vol. **7**, no. 3,
[21] Nasab M J and Asakereh A, "A Review of Methods of Increasing the Efficiency of Stone Columns to Ground Improvement," *International Journal of Science Engineering Investigations*, 2015,vol. **4**, no. 11, pp. 75-8.